# Carbon dioxide reforming of methane over co-precipitated Ni–Ce–$ZrO_2$ catalysts

H.S. Potdar, Hyun-Seog Roh, Ki-Won Jun *, Min Ji and Zhong-Wen Liu

*Chemical Technology Division, Korea Research Institute of Chemical Technology, P.O. Box 107, Yuseong, Daejeon 305-600, Korea*

Received 5 June 2002; accepted 8 August 2002

An active and relatively stable Ni–Ce–$ZrO_2$ catalyst has been designed and prepared conveniently by a novel one-step co-precipitation/digestion method. This catalyst exhibited higher stability compared with a catalyst having the same composition but prepared using the conventional impregnation method. It was found that 15% Ni (w/w) co-precipitated with Ce–$ZrO_2$ making the cubic phase of $Ce_{0.8}Zr_{0.2}O_2$ gave synthesis gas with $CH_4$ conversion more than 97% at 800 °C and that the activity was maintained for 100 h during the reaction. The higher activity, conversion and stability of these catalysts are mainly related to the nano-crystalline nature of cubic $Ce_{1-x}Zr_xO_2$ producing strong interaction with finely dispersed nano-sized $NiO_x$ crystallites.

**KEY WORDS:** co-precipitation/digestion; cubic $Ce_{1-x}Zr_xO_2$; $CH_4$; $CO_2$; Ni; reforming.

## 1. Introduction

During the last decade, the $CO_2$ reforming of $CH_4$ (CDR) has received much attention for the production of synthesis gas as a complementary process over the well-established steam-reforming process because of both environmental and commercial reasons [1,2]. Nickel-based catalysts on various support materials showed high activity in this reaction comparable to noble metals [3–6]. However, Ni catalysts easily deactivate by coke formation and/or sintering of the metallic and support phases [4,6,7].

Recently, there has been interest in mixed oxide catalyst systems containing $CeO_2$–$ZrO_2$ [8]. It has been reported that the addition of $ZrO_2$ to $CeO_2$ leads to improvements in the oxygen storage capacity of $CeO_2$, the redox property, thermal resistance and promotion of metal dispersion [8–10], resulting in better performance in certain reactions such as CO oxidation [11] and combustion of methane [12]. This was found to be due to the partial substitution of $Ce^{4+}$ with $Zr^{4+}$ in the lattice of $CeO_2$, which results in a solid solution formation [9]. Because of better thermal stability as well as their enhanced oxygen mobility, the $Ce_{1-x}$–$Zr_xO_2$ system has appeared as a promising candidate to be used as a support material in nickel-based catalyst systems. Only a limited number of papers have been concerned with this objective [13–15]. Lercher *et al.* [6] have reported that Pt/$ZrO_2$ showed excellent performance in CDR. However, Ni/$ZrO_2$ with a high Ni loading is not viable for CDR due to coke formation. Li *et al.* [16,17] have reported that Ni/$ZrO_2$ catalysts with more than 10 wt% Ni loading showed high activity at 750 °C for 30 h in CDR despite producing a large amount of carbon. However, its stable activity can be obtained only under diluted reaction conditions, namely dilution of reactants with $N_2$ and dilution of catalysts with quartz sand. Previously, Ni catalysts supported on a tetragonal Ce–$ZrO_2$, prepared by the molten salt method, were applied to steam reforming of methane (SRM) [18,19], oxy-reforming of methane (ORM) [20,21], and oxy-SRM (OSRM) [18,21]. Montoya *et al.* [22] applied Ni supported on a tetragonal $CeO_2$–$ZrO_2$ support for the CDR reaction; however, the problem of support sintering at 800 °C could not be avoided completely.

It has been reported that the cubic phase of $CeO_2$–$ZrO_2$ has more oxygen storage capacity and is more easily reducible than the tetragonal phase [7,23]. It is also known that Ni dispersion using the co-precipitation method is higher than that employing the conventional impregnation method [9]. To the best of our knowledge, cubic $Ce_{0.8}Zr_{0.2}O_2$ support containing nickel has not yet been tried in the CDR reaction. In the work described in this paper, a novel one-step chemical co-precipitation/digestion method was used to prepare a nickel-based catalyst on a cubic $Ce_{0.8}Zr_{0.2}O_2$ support for evaluation in CDR.

## 2. Experimental

Cubic $Ce_{0.8}Zr_{0.2}O_2$ catalysts with varying NiO concentrations were prepared by a one-step co-precipitation/digestion method. Stoichiometric quantities of zirconyl nitrate solution (20 wt% in $ZrO_2$ base, MEL

* To whom correspondence should be addressed.

1011-372X/02/1100-0095/0 

Chemicals), cerrous nitrate (99.9%, Aldrich) and nickel nitrate (97%, Junsei Chemicals) were dissolved in distilled water, and the resulting solution was transferred to a round-bottomed flask. To this solution an aqueous solution of 20% KOH (w/w) was added drop-wise at 80 °C with constant stirring to attain an alkaline pH (9.5–10.5). During the entire course of co-precipitation reactions, the pH was maintained in this alkaline range. The precipitates were digested at 80 °C for 72 and 96 h. Later, they were thoroughly washed with distilled water several times to remove any potassium impurity and then initially air-dried for 48 h followed by drying at 120 °C for 6 h. The dried mass thus obtained was then finely ground to a particle size less than a micron. This material was finally calcined at 500 °C for 6 h in an aerobic environment to get the final catalyst material. Many synthesis parameters such as pH, digestion time, addition sequence and use of tetrapropyl ammonium bromide, *i.e.*, TPABr (4.3% by weight), were systematically varied. This was done to optimize conditions in order to get high surface area in 30% Ni loaded (w/w) on cubic $Ce_{0.8}Zr_{0.2}O_2$ material after calcination at 500 °C for 6 h. Furthermore, Ni content was gradually varied from 5 to 15% in the $Ce_{0.8}Zr_{0.2}O_2$ supports in order to optimize the Ni loading. Simultaneously, for comparison, a $Ce_{0.8}Zr_{0.2}O_2$-supported Ni catalyst system with optimized Ni loading (15%, w/w) was prepared by the conventional impregnation method. This was achieved by impregnating appropriate amounts of $Ni(NO_3)_2{\cdot}6H_2O$ onto cubic supports of $Ce_{0.8}Zr_{0.2}O_2$ (prepared by the co-precipitation methodology described previously), followed by drying at 100 °C and later calcining the material at 800 °C for 6 h in air. Similarly, a $Ce_{0.8}Zr_{0.2}O_2$-supported 15% Ni catalyst system was also prepared by calcining the one-step co-precipitated material at 800 °C for 6 h in air.

The BET specific surface area was measured by nitrogen adsorption at −196 °C using a Micromeritics (ASAP-2400) surface area measurement apparatus. The XRD patterns were recorded using a Rigaku 2155D6 diffractometer (Ni filtered Cu $K_\alpha$ radiation, 40 kV, 50 mA). Pulse chemisorptions were performed in a multifunction apparatus. About 250 mg of catalyst was placed in a quartz reactor. Before pulse chemisorption, the sample was reduced in 5% $H_2$/Ar at 700 °C for 3 h. Then the sample was purged in Ar at 720 °C for 1 h and cooled to 50 °C in flowing Ar. Hydrogen was pulsed over the catalyst to measure the chemisorption at 50 °C using 5% $H_2$/Ar and continued at 8 min intervals until the area of the hydrogen peak on the chromatograph was identical. Based on the hydrogen uptake, the surface area of Ni was calculated by assuming the adsorption stoichiometry of one hydrogen atom per nickel surface atom ($H/Ni_s = 1$).

Activity tests were carried out using a fixed-bed microreactor [18]. The reactant feed comprised a gaseous mixture of $CH_4:CO_2:N_2$ (1.00:1.04:1.00). $N_2$ was employed as the reference for calculating $CH_4$ and $CO_2$ conversion. Each catalyst was reduced in the reactor with 5% $H_2/N_2$ at 700 °C for 2 h prior to each catalytic measurement. The CDR reaction was tested at 800 °C. Effluent gases from the reactor were analyzed by a Chrompack CP9001 gas chromatograph (fitted with a fused silica capillary column (CarboPLOT P7)) equipped with a thermal conductivity detector (TCD).

## 3. Results and discussion

### 3.1. Synthesis and catalyst characterization

An aim of the present study was to optimize the preparation parameters in a one-step co-precipitation/digestion methodology toward the co-precipitation of nickel, cerium and zirconium hydroxides, and thus obtain a novel NiO dispersed cubic $Ce_{0.8}Zr_{0.2}O_2$ matrix with high surface area. Another aspect of this work was to evaluate the performance of the catalyst systems in the CDR reaction for elevated time periods in order to test catalyst stability.

Table 1 summarizes characteristics of the supports and catalysts prepared by the one-step co-precipitation/digestion after the calcination step at 500 °C for 6 h in static air. The highest surface area (181 $m^2$ g) was obtained at a pH of 10.5. However, if the pH is 9.5, then the surface area decreases to 62.3 $m^2$ g. The increase in digestion time from 72 to 96 h resulted in lowering the surface area from 181 to 154 $m^2$ g. The addition of TPABr and reverse addition of cationic solution to the precipitant are not beneficial to improving the surface area. Hence, the optimized reaction condition to obtain high surface area materials is achieved by the addition of 20% precipitant, viz. aqueous KOH, to an aqueous solution containing stoichiometric concentrations of cerium, zirconium and nickel nitrates for a digestion time of 72 h at 80 °C.

For a comparison of the surface area of the various catalytic materials, samples of cubic $Ce_{0.8}Zr_{0.2}O_2$ and $CeO_2$ were synthesized by the one step co-precipitation/digestion methodology described above. It was observed that the surface area of $Ce_{0.8}Zr_{0.2}O_2$ was 115 $m^2$ g, whereas that of $CeO_2$ was 112 $m^2$ g after calcination at 500 °C for 6 h. The surface-area values are quite comparable with reported data for similar compositions prepared by other chemical routes such as a sol-gel, hydrothermal, microwave hydrothermal, micro-emulsion and high-energy ball milling [3,24,25].

In order to understand the phase composition, crystallinity and size of crystallites in these materials, XRD patterns of the 30% Ni on cubic $Ce_{0.8}Zr_{0.2}O_2$ samples were obtained (figure 1). All the patterns showed reflections typical of the cubic fluorite structure of $Ce_{0.8}Zr_{0.2}O_2$ corresponding to the (111), (200), (311), (222) and (400) planes. The lines corresponding to

Table 1
Characteristics of supports and catalysts after calcination in air at 500 °C for 6 h.

| Code | Ni content (%) | Support | pH | Surf. area ($m^2/g$) [d] | Ce–$ZrO_2$ size (nm) | NiO size (nm) | Lattice parameter: $a_0$ (Å) |
|---|---|---|---|---|---|---|---|
| 1 | 30 | Ce–$ZrO_2$ | 9.5 | 63 | 16.8 | 22.7 | 5.35 |
| 2 [f] | 30 | Ce–$ZrO_2$ | 10.5 | 181 | 6.2 | 3.4 | 5.35 |
| 3 [a] | 30 | Ce–$ZrO_2$ | 10.5 | 154 | 6.7 | 3.4 | 5.35 |
| 4 [b] | 30 | Ce–$ZrO_2$ | 10.5 | 159 | 6.2 | 3.4 | 5.35 |
| 5 [c] | 30 | Ce–$ZrO_2$ | 10.5 | 133 | 6.2 | 3.4 | 5.35 |
| 6 | 0 | Ce–$ZrO_2$ | 10.5 | 115 | 6.2 | – | 5.35 |
| 7 | 0 | $CeO_2$ | 10.5 | 112 | 6.8 | – | 5.41 |
| 8 [f] | 5 | Ce–$ZrO_2$ | 10.5 | 125 | 9.5 | NA [e] | 5.35 |
| 9 [f] | 10 | Ce–$ZrO_2$ | 10.5 | 127 | 5.5 | NA [e] | 5.35 |
| 10 [f] | 15 | Ce–$ZrO_2$ | 10.5 | 144 | 8.2 | NA [e] | 5.35 |

(Conditions: digestion time = 72 h; addition of KOH → cation solution).
[a] Digestion time = 96 h.
[b] TPABr was added.
[c] Reverse addition (cation solution → KOH).
[d] Accuracy = ±0.5.
[e] Not available due to very broad and weak XRD peaks.
[f] These catalysts were examined for CDR.

either $ZrO_2$ or $CeO_2$ are not observed. This observation indicates formation of $Ce_{0.8}Zr_{0.2}O_2$ at this temperature without any unreacted $ZrO_2$ or $CeO_2$ as an impurity phase. This is also indicative of the fact that Ce and Zr ions are homogeneously mixed. Furthermore, the calculated lattice parameter $a_0$ of 5.35 Å agrees well with the reported lattice parameter of $Ce_{0.8}Zr_{0.2}O_2$, confirming thereby the formation of the cubic phase in the present case [5,26,27]. The lattice parameter $a_0$ was calculated from a slow scan using the equation as given below:

$$\sin^2\theta(hkl) = \lambda^2(h^2 + k^2 + l^2)/4a_0^2. \quad (1)$$

The (200) reflection appearing at $2\theta = 33.453^0$ was used for calculation of the lattice parameter. The crystallite size in the various materials was estimated using the Debye–Scherrer equation:

$$D_{hkl} = 0.9\lambda/\beta_{hkl}\cos\theta \quad (2)$$

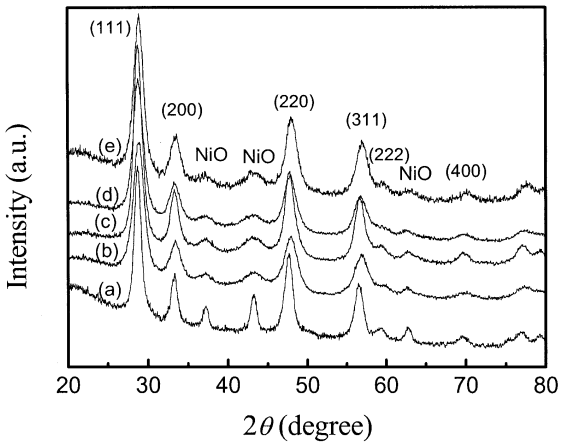


Figure 1. XRD patterns of co-precipitated 30% Ni dispersed on cubic $Ce_{0.8}Zr_{0.2}O_2$ catalysts ((a) code 1; (b) code 2; (c) code 3; (d) code 4; and (e) code 5 in table 1).

where $D_{hkl}$ is the crystallite size, $\lambda$ is the wavelength of Cu $K_\alpha$ radiation, $\beta_{hkl}$ is the peak width at half maximum and $\theta$ is the Bragg diffraction angle. The calculated crystallite sizes of $Ce_{0.8}Zr_{0.2}O_2$ were found to be in the range of 6.2–6.7 nm except for the sample prepared at a pH of 9.5 (16.8 nm). Presumably, this is why the surface area of this sample is lower (63 $m^2$ g). The other reflections observed at $2\theta$ values equal to 37.21, 43.21, 62.73 and 75.42 degrees are assigned to cubic NiO with $a_0 = 4.176$ Å [28]. The crystallite size of NiO in the code 1 sample (22.7 nm) is higher than that of other materials prepared at a pH of 10.5, which is nearly 3.4 nm. This indicates that pH is an important parameter for the synthesis of nano-crystalline Ni–Ce–$ZrO_2$ using the co-precipitation method. Thus, XRD and BET surface area measurements confirmed that high surface area and smaller crystallite sizes are obtained at pH = 10.5, digestion time = 72 h, and the addition of 20% (w/w) aqueous solution of KOH to the cationic solution containing Ce, Zr and Ni nitrates.

Because 30% Ni dispersed on $Ce_{0.8}Zr_{0.2}O_2$ (code 2 in table 1) showed the highest surface area and the lowest crystallite size, this catalyst was employed for CDR. However, the catalyst deactivated with time on stream (as discussed in the next section) due to sintering of Ni particles and/or coke formation. Therefore, in order to rectify the sintering problem, the Ni content in materials was varied from 5 to 15% using the co-precipitation/digestion method. On doing so, the surface area in these materials was observed to increase from 125 $m^2$ g to 144 $m^2$ g with an increase in Ni content. The XRD patterns for these are shown in figure 2. The XRD pattern of co-precipitated $CeO_2$ is also included for comparison sake. The results indicate a shift in the reflections for all peaks toward higher angles due to the insertion of $Zr^{4+}$ ions in the lattice of $CeO_2$. The XRD patterns clearly

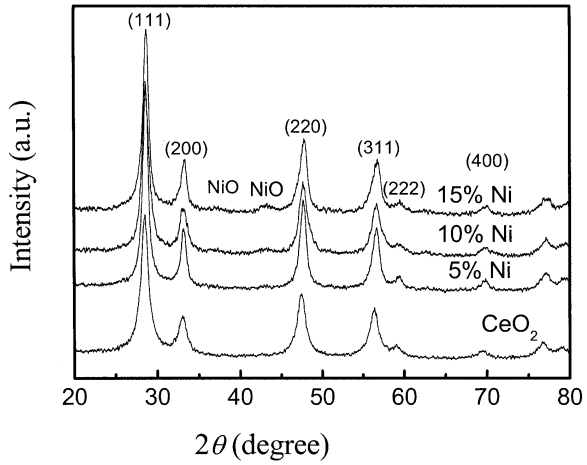


Figure 2. XRD patterns of co-precipitated $CeO_2$ and cubic Ni–Ce–$ZrO_2$ catalysts with different Ni loadings.

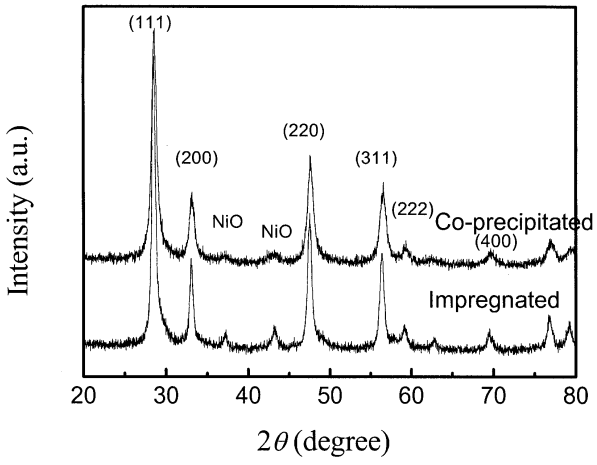


Figure 3. XRD patterns of co-precipitated and impregnated Ni–Ce–$ZrO_2$ catalysts (Ni loading = 15%).

indicate the presence of cubic $Ce_{0.8}Zr_{0.2}O_2$ phase having better dispersion of cubic NiO particles compared with 30% Ni dispersed on $Ce_{0.8}Zr_{0.2}O_2$ (see figure 1). The estimated $Ce_{0.8}Zr_{0.2}O_2$ sizes of the samples of 5, 10 and 15% Ni contents are 9.5, 5.5 and 8.2 nm, respectively. However, the NiO peaks are so broad that NiO crystallite size cannot be obtained, which indicates that these catalysts have better dispersion of fine cubic NiO phase in the $Ce_{0.8}Zr_{0.2}O_2$ matrix than the 30% Ni catalyst. Ni–Ce–$ZO_2$ catalysts with various Ni loadings prepared by the co-precipitation method were tested for CDR, as described in the next section. However, it was found that these catalysts also deactivated during the test of 35 h due to sintering of Ni particles.

To address this problem, therefore, this catalyst was made by calcination at 800 °C for 6 h in air to improve its thermal stability by increasing the interaction between Ni and cubic $Ce_{0.8}Zr_{0.2}O_2$. It is expected that Ni sintering and carbon formation can be prevented due to the strong Ni-support interactions. As a comparison, 15% Ni catalyst loaded on $Ce_{0.8}Zr_{0.2}O_2$ made by the conventional impregnation method was also calcined at the same temperature and for the same duration in air. Table 2 summarizes the characteristics of the co-precipitated and impregnated catalysts. The surface areas of co-precipitated and impregnated catalysts after calcination at 800 °C for 6 h were found to be 80 and 50 $m^2/g$, respectively. The XRD patterns for these catalysts are depicted in figure 3. The crystallite size of the impregnated support material was found to be higher (18 nm) than that of co-precipitated support material (13 nm). The lattice parameter ($a_0$) for both materials was found to be 5.35 Å. However, the NiO peaks in the co-precipitated catalyst are much broader than those in the impregnated one (8.5 nm), indicating thereby better dispersion and less sintering of fine NiO particles during the calcination process. The values of $H_2$ uptake of the co-precipitated and impregnated catalysts obtained by calcination at 800 °C for 6 h were found to be 20.92 and 7.44 $\mu$mol/$g_{cat}$. The Ni surface areas for both samples are also given in table 2. For the impregnated catalyst, the $H_2$ uptake and Ni surface area were lower than those of the co-precipitated catalyst. After reduction treatment, the crystallite sizes for $Ce_{0.8}Zr_{0.2}O_2$ of the impregnated and co-precipitated catalysts were found to be 18.2 and 12.2 nm, respectively.

Table 2
Comparison of characteristics between co-precipitated and impregnated catalysts after calcination at 800 °C for 6 h.

| | Co-precipitated | Impregnated |
|---|---|---|
| BET surface area ($m^2/g$) [a] | 80 | 50 |
| Crystallite size of support (nm) [b] | 13 | 18 |
| Crystallite size of NiO (nm) [b] | NA [d] | 8.5 |
| Lattice parameter of NiO (Å) [b] | 4.17 | 4.17 |
| Ni surface area ($m^2/g$) [c] | 1.71 | 0.61 |

[a] Estimated from $N_2$ adsorption at −196 °C.
[b] Estimated from XRD.
[c] Estimated from $H_2$ adsorption at 50 °C for the reduced catalyst.
[d] Not available due to very broad and weak XRD peaks.

### 3.2. Catalytic performance

Because 30% Ni dispersed on $Ce_{0.8}Zr_{0.2}O_2$ (code 2 in table 1) showed the highest surface area and the lowest crystallite size, this catalyst was employed for CDR. The reaction data are shown in figure 4. The $CH_4$ and $CO_2$ conversion were nearly equal to 96% up to 14 h time on stream and then decreased due to sintering of Ni particles and/or coke formation.

To find out the optimum Ni loading, Ni–Ce–$ZrO_2$ catalysts with various Ni loadings prepared by the co-precipitation method were tested for CDR (figure 5). The 5% and 10% Ni catalysts showed lower $CH_4$ and $CO_2$ conversion (less than 85%). On the other hand, 15% Ni catalyst showed conversions higher than 95%. This catalyst slowly deactivated during the test of 35 h

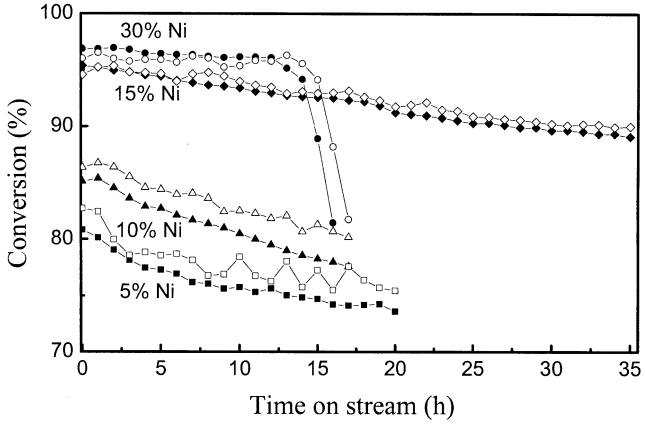


Figure 4. $CH_4$ and $CO_2$ conversion with time on stream over co-precipitated Ni–Ce–$ZrO_2$ catalysts with various Ni loadings in CDR (reaction conditions: $T = 800\,^{\circ}C$, $CH_4 : CO_2 : N_2 = 1.00 : 1.04 : 1.00$, GHSV = 108 000 ml/h $g_{cat}$; solid symbol: $CH_4$ conversion; hollow symbol: $CO_2$ conversion).

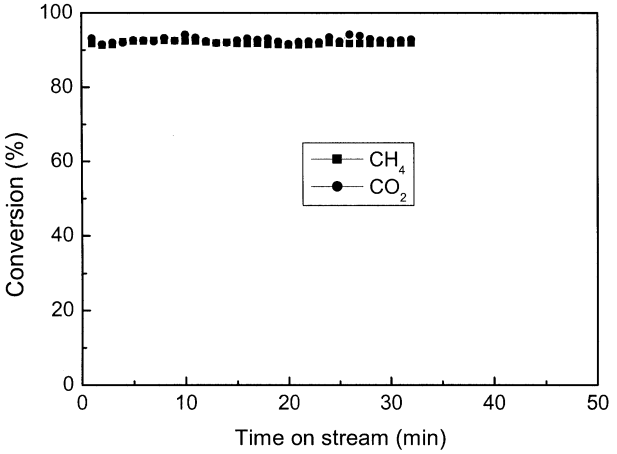


Figure 6. $CH_4$ and $CO_2$ conversion with time on stream over co-precipitated Ni–Ce–$ZrO_2$ catalyst in CDR (Ni loading = 15%; reaction conditions: $T = 800\,^{\circ}C$, $CH_4 : CO_2 : N_2 = 1.00 : 1.04 : 1.00$, GHSV = 216 000 ml/h $g_{cat}$).

due to sintering of Ni particles. However, it showed relatively high and stable activity among the catalysts tested; 15% Ni loading was selected for the next step.

To improve its thermal stability by increasing the interaction between Ni and cubic $Ce_{0.8}Zr_{0.2}O_2$, this catalyst was re-calcined at 800 °C for 6 h in air because of the fact that Ni sintering and carbon formation can be prevented due to the strong Ni-support interactions. As a comparison, 15% Ni catalyst loaded on $Ce_{0.8}Zr_{0.2}O_2$ made by the conventional impregnation method was also calcined at the same temperature and for the same duration in air. The $CO_2$ reforming reaction data on both catalysts are presented in figure 5. The impregnated catalyst showed an initial conversion of 80% (both $CH_4$ and $CO_2$ conversion). However, it decreased to 65% within 2 h. The $CO_2$ conversion was slightly higher than $CH_4$ conversion due to reverse water–gas shift reaction (RWGS). On the other hand, the co-precipitated catalyst showed conversion (both $CH_4$ and $CO_2$) of more than 97% up to 100 h without significant deactivation. For this catalyst, the $CH_4$ conversion was slightly higher than $CO_2$ conversion due to the fact that the feed ratio of $CO_2/CH_4 = 1.04$ and possibly experimental error (GC error <2%). Thus, the co-precipitated/digested catalyst gave a better performance than the conventional impregnated one. To the best of our knowledge, it is a very rare case that supported Ni catalyst having more than 5% Ni shows such high activity and stability for 100 h under the condition of GHSV = 100 800 ml/h $g_{cat}$ in CDR. Since the co-precipitated Ni–Ce–$ZrO_2$ exhibited almost equilibrium values of $CH_4$ and $CO_2$ conversion, GHSV was doubled (216 000 ml/h $g_{cat}$) to avoid equilibrium limited condition and the results are shown in figure 6. Even though GHSV was doubled, high $CH_4$ conversion (92%) and $CO_2$ conversion (93%) were still obtained and the stability was maintained for 32 h. Thus, it was confirmed that co-precipitated Ni–Ce–$ZrO_2$ catalyst shows high activity and stability even under non-equilibrium limited condition. It is most likely that the higher catalytic performance is related to the high surface area, the nano-crystalline nature of the cubic $Ce_{0.8}Zr_{0.2}O_2$ support, the better dispersion of fine NiO particles in the $Ce_{0.8}Zr_{0.2}O_2$ support and their interaction with the support material and high Ni surface area.

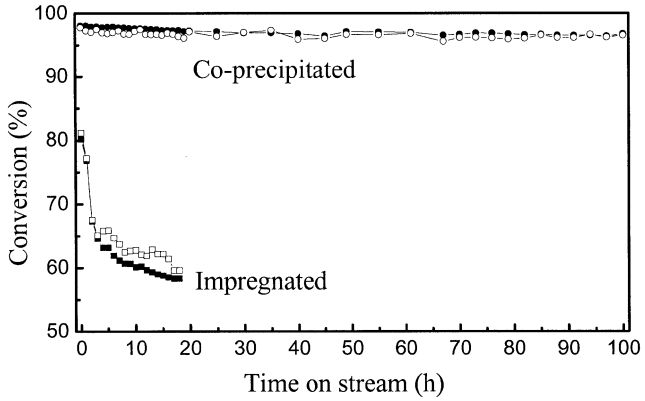


Figure 5. $CH_4$ and $CO_2$ conversion with time on stream over co-precipitated and impregnated Ni–Ce–$ZrO_2$ catalysts in CDR (Ni loading = 15%; reaction conditions: $T = 800\,^{\circ}C$, $CH_4 : CO_2 : N_2 = 1.00 : 1.04 : 1.00$, GHSV = 108 000 ml/h $g_{cat}$; solid symbol: $CH_4$ conversion; hollow symbol: $CO_2$ conversion).

## 4. Discussion

The enhanced conversion and thermal stability in the co-precipitated Ni–Ce–$ZrO_2$ catalyst in CDR are explained as follows: The high surface area in the co-precipitated material is maintained due to agglomeration of primary particles during digestion and strengthening of the network structure, giving a porous material which is capable of withstanding thermal treatment [29]. This allows the high surface area to be retained

even after calcination at 800 °C in air compared to the impregnated catalyst. The ability of the cubic $Ce_{0.8}Zr_{0.2}O_2$ solid solution is related to its rapid reduction/oxidation capability by shifting between $CeO_2$ under oxidizing conditions and $Ce_2O_3$ under reducing conditions. The capability of the redox couple $Ce^{4+}$–$Ce^{3+}$ is reported to be enhanced in the cubic solid solution of $Ce_{1-x}$–$Zr_xO_2$ [8]. In addition, the cubic solid solution is more reducible than the tetragonal solid solution [11]. Furthermore, oxygen storage capacity/mobility is favored in the cubic structure rather than in the tetragonal structure [8,11]. The novel method of co-precipitation/digestion helps to produce a nano-sized $Ce_{0.8}Zr_{0.2}O_2$ matrix with fine $NiO_x$ crystallites strongly interacting with the support in a single step. From the various characterization results discussed in the previous section, the reaction results are explained using a reported mechanism [3]. The decomposition of methane first occurs on the fine nickel particles, resulting in the formation of hydrogen and carbon. Simultaneously, the reaction of carbon with oxygen occurs to produce CO. The required oxygen is available from the cubic $Ce_{0.8}Zr_{0.2}O_2$ support with high oxygen mobility near the metal particles or from the decomposition of $CO_2$ [3]. In this dual path mechanism [30,31], the role of support is equally important in dissociative adsorption of $CO_2$ [3] near the metal particles, which help in transferring oxygen to coked metal. In this way the removal of carbon is accelerated and the stability of the catalyst during the CDR is maintained.

## 5. Conclusions

A novel one-step co-precipitation/digestion process produced 15% Ni loaded on cubic $Ce_{0.8}Zr_{0.2}O_2$ catalyst having better activity and thermal stability than impregnated catalyst having same composition. The higher activity and stability of this catalyst system in CDR is mainly related to the high surface area, the nano-sized nature of the cubic $Ce_{0.8}Zr_{0.2}O_2$ support and the better dispersion of fine NiO particles in the $Ce_{0.8}Zr_{0.2}O_2$ matrix and their strong interaction with support material.

## Acknowledgment

H.S. Potdar is grateful to KISTEP, Korea for a fellowship.

## References

[1] M.C.J. Bradford and M.A. Vannice, Catal. Rev.-Sci. Eng. 41 (1999) 1.
[2] J.R. Rostrup-Nielsen, Stud. Surf. Sci. Catal. 81 (1993) 25.
[3] S.M. Stagg-Williams, F.B. Noronha, G. Fendley and D.E. Resasco, J. Catal. 194 (2000) 240.
[4] J.R. Rostrup-Nielsen and J.H. Bak Hansen, J. Catal. 144 (1993).
[5] M.E.S. Hegarty, A.M. O'Connor and J.R.H. Ross, Catal. Today 42 (1998) 225.
[6] J.A. Lercher, J.H. Bitter, W. Hally, W. Niessen and K. Seshan, Stud. Surf. Sci. Catal. 101 (1996) 463.
[7] S. Wang and G.Q. Lu, Appl. Catal. A 169 (1998) 271.
[8] Trovarelli, C. de Leitenburg and G. Dolcetti, Chemtech June (1997) 32.
[9] J. Kaspar, P. Fornasiero and M. Graziani, Catal. Today 50 (1999) 285.
[10] S. Rossignol, F. Gerard and D. Duprez, J. Mater. Chem. 9 (1999) 1615.
[11] M. Thammachart, V. Meeyoo, T. Risksomboon and S. Osuwan, Catal. Today 68 (2001) 53.
[12] C. Bozo, N. Guilhaume, E. Garbowski and M. Primet, Catal. Today 594 (2000) 33.
[13] C. de Leitenburg, A. Trovarelli, J.L. Lorea, F. Cavani and G. Bini, Appl. Catal. A 139 (1996) 161.
[14] E. Bekyarova, P. Fornasiero, J. Kaspar and M. Graziani, Catal. Today 45 (1998) 178.
[15] D. Terribile, A. Trovarelli, C. de Leitenburg, A. Primareva and G. Dolcetti, Catal. Today 47 (1999) 133.
[16] X. Li, J.-S. Chang and S.-E. Park, Chem. Lett. (1999) 1099.
[17] X. Li, J.-S. Chang, M. Tian and S.-E. Park, Appl. Organometal. Chem. 15 (2001) 109.
[18] H.-S. Roh, K.-W. Jun, W.-S. Dong, S.-E. Park and Y.-S. Baek, Catal. Lett. 74 (2001) 31.
[19] H.-S. Roh, K.-W. Jun, W.-S. Dong, J.-S. Chang, S.-E. Park and Y.-I. Joe, J. Mol. Catal. A 181 (2002) 137.
[20] H.-S. Roh, W.-S. Dong, K.-W. Jun and S.-E. Park, Chem. Lett. (2001) 88.
[21] W.-S. Dong, H.-S. Roh, K.-W. Jun, S.-E. Park and Y.-S. Oh, Appl. Catal. A 226 (2002) 63.
[22] J.A. Montoya, E. Romero-Pascual, C. Gimon, P.D. Angel and A. Monzon, Catal. Today 63 (2000) 71.
[23] S. Rossignol, Y. Madier and D. Duprez, Catal. Today 509 (1999) 261.
[24] Cabanas, J.A. Darr, E. Lester and M. Poliakoff, J. Mater. Chem. 11 (2001) 561.
[25] H.S. Potdar, S.B. Deshpande, A.S. Deshpande, S.P. Gokhale, Y.B. Khollam, A.J. Patil and S.K. Date, Mater. Chem. Phys. 74 (2001) 306.
[26] G. Colon, M. Pijolat, F. Valdivieso, H. Vidal, J. Kaspar, E. Fiocchio, M. Daturi, C. Binet, J.C. Lavalley, P.T. Bakar and S. Bernal, J. Chem. Soc. Faraday Trans. 94 (1998) 3717.
[27] G. Balducci, M.S. Islam, J. Kaspar, P. Fornasiero and M. Grazini, Chem. Mater. 12 (2000) 677.
[28] ASTM Card No: 4-0835.
[29] G.K. Chuan and S. Jaenicke, Appl. Catal. A 163 (1997) 261.
[30] F.B. Noronha, E.C. Fendley, R.R. Soares, W.E. Alvarez and D.E. Resasco, Chem. Eng. J. 82 (2001) 21.
[31] G.S. Zafiris and R.J. Gorte, J. Catal. 143 (1993) 86.